Journal of Environmental Management 222 (2018) 86–94

Contents lists available at ScienceDirect

Journal of Environmental Management

journal homepage: www.elsevier.com/locate/jenvman

Research article

Interannual variations in surface urban heat island intensity and associated drivers in China

Rui Yao[a,e], Lunche Wang[a,e,*], Xin Huang[b,c,**], Wenwen Zhang[a], Junli Li[d], Zigeng Niu[a,e]

[a] Laboratory of Critical Zone Evolution, School of Earth Sciences, China University of Geosciences, Wuhan 430074, China
[b] School of Remote Sensing and Information Engineering, Wuhan University, Wuhan 430079, China
[c] State Key Laboratory of Information Engineering in Surveying, Mapping and Remote Sensing, Wuhan University, Wuhan 430079, China
[d] School of Resource and Environment, Anhui Agricultural University, Hefei 230036, China
[e] Hunan Key Laboratory of Remote Sensing of Ecological Environment in Dongting Lake Area, China

ARTICLE INFO

Keywords:
Surface urban heat island
Climate variability
Urbanization
Interannual
China

ABSTRACT

The spatial, diurnal and seasonal variations of surface urban heat islands (SUHIs) have been investigated in many places, but we still have limited understanding of the interannual variations of SUHIs and associated drivers. In this study, the interannual variations in SUHI intensity (SUHII, derived from MODIS land surface temperature (LST) data (8-day composites of twice-daily observations), urban LST minus rural) and their relationships with climate variability and urbanization were analyzed in 31 cities in China for the period 2001–2015. Significant increasing trends of SUHII were observed in 71.0%, 58.1%, 25.8% and 54.8% the cities in summer days (SDs), summer nights (SNs), winter days (WDs) and winter nights (WNs), respectively. Pearson's correlation analyses were first performed from a temporal perspective, which were different from a spatial perspective as previous studies. The results showed that the SUHII in SDs and WDs was negatively correlated with the background LST and mean air temperature in most of the cities. The nighttime SUHII in most cities was negatively and positively correlated with total precipitation and total sunshine duration, respectively. Average wind speed has little effect on SUHII. Decreasing vegetation and increased population were the main factors that contributed to the increased SUHII in SDs and SNs, while albedo only influenced the SUHII in WDs. In addition, Pearson's correlation analyses across cities showed that cities with higher decreasing rates of vegetation exhibited higher increasing rates of the SUHII in SDs and WDs. Cities with larger population growth rates do not necessarily have higher increasing rates of SUHII.

1. Introduction

Urbanization is accelerating worldwide, especially in developing countries (United Nations, 2014). Urban heat islands (UHIs) (Zhou et al., 2014), air pollution (Tao et al., 2016) and other problems due to urbanization are becoming increasingly serious and generating increasing attentions globally. Comprehensive analyses of urbanization effects on the environment are needed.

UHI, a major harmful consequence of urbanization, refers to higher temperatures in urban areas than in nonurban areas (Zhou et al., 2014; Giorgio et al., 2017). UHIs have a series of adverse impacts on ecosystems (e.g. net primary production (Imhoff et al., 2004)), human health (e.g. aggravating respiratory disease and even leading to death (Curriero et al., 2002)) and the environment (e.g. air and water pollution (Grimm et al., 2008)). UHIs estimated via remote sensing are called surface UHI (SUHI), which is different from weather station based air UHI in terms of conception, magnitude and application (Voogt and Oke, 2003). SUHI has attracted considerable attentions in recent decades due to the easy access, wide and full coverage of remote sensing (Zhou et al., 2014; Liu and Zhang, 2011). Moderate Resolution Imaging Spectroradiometer (MODIS) Land surface temperature (LST) data have 1 km spatial resolution with (at best) twice daily temporal resolution and wide coverage, and have been used to study the spatial, diurnal and seasonal variations of SUHI throughout world (Han and Xu, 2013; Hung et al., 2006; Zhang et al., 2004; Zhou et al., 2013, 2016b; Imhoff et al., 2010; Clinton and Gong, 2013; Peng et al., 2012; Yao et al., 2017a). In China, the daytime SUHI intensity (SUHII, the LST in urban area minus in rural area) exhibited great spatial and seasonal heterogeneity: a) it differed largely by cities, ranging from −1 K in Lanzhou to more than 7 K in Kunming (Wang et al., 2015b), b) it

* Corresponding author. Laboratory of Critical Zone Evolution, School of Earth Sciences, China University of Geosciences, Wuhan 430074, China.
** Corresponding author. Laboratory of Critical Zone Evolution, School of Earth Sciences, China University of Geosciences, Wuhan 430074, China.
E-mail addresses: wang@cug.edu.cn (L. Wang), huang_whu@163.com (X. Huang), lijunli866@ahau.edu.cn (J. Li).

https://doi.org/10.1016/j.jenvman.2018.05.024
Received 8 January 2018; Received in revised form 5 April 2018; Accepted 9 May 2018
Available online 25 May 2018
0301-4797/

differed greatly in seasons, the highest and lowest SUHII were normally in summer and winter, respectively (Wang et al., 2015b; Zhou et al., 2014, 2016a; 2016b; Yao et al., 2017c). The nighttime SUHII did not change substantially across cities and seasons (Wang et al., 2015b; Zhou et al., 2014, 2016a; 2016b; Yao et al., 2017c). The air UHI intensity also varied spatially and seasonally in China, though it was much lower than SUHII (Wang et al., 1990; Hua et al., 2008).

However, with rapid urbanization, few studies have analyzed the interannual variations of SUHIs at a national scale due to short time series of the MODIS LST data (available from 2000 to present). Zhou et al. (2016a) showed that the SUHII increased in about one-third of the 32 cities in China during 2003–2012; Yao et al. (2017c) showed that the SUHII increased in approximately half of the 31 cities in China during 2001–2015, yet no more information about the SUHII variability is available. Therefore, more studies focusing on the interannual variations in SUHII in China were needed.

The relationships between diurnal, seasonal, spatial variations of SUHIs and the associated factors have been studied thoroughly, and the daytime and nighttime SUHII were strongly linked to vegetation activity (in growing seasons) and albedo (Peng et al., 2012; Xian and Crane, 2006; Wang et al., 2017). Anthropogenic heat release, air temperature, precipitation and wind speed also influence the SUHII, while population density contribute less (Du et al., 2016; Peng et al., 2012). However, the relationships between interannual variations in SUHII and its associated factors may not necessarily be consistent with the relationships between spatial variations in SUHII and related drivers. Previous studies only analyzed the interannual variations in SUHII and its relationships with no more than three factors, for example, Zhou et al. (2016a) showed that the interannual variations in SUHII were generally invariant with mean air temperature and precipitation; Yao et al. (2017a) showed that decreased vegetation was an important for the increasing SUHII in China's Yangtze River Basin; Yao et al. (2017c) showed that increasing anthropogenic heat release and decreased vegetation were the main factors for the increasing SUHII in China, and the daytime SUHII was negatively correlated with background LST. Thus, ignoring other factors (e.g. sunshine duration, wind speed, albedo and population) may miss important drivers. Much more detailed analysis should be conducted for clear understanding.

Therefore, the present study aims at filling the existing research gaps and improving our understanding of the relationships between interannual variations in SUHII and related drivers. We performed systematic analyses of a) the interannual variations of SUHII, b) its relationships with climate factors (mean air temperature, background LST, total precipitation, total sunshine duration and average wind speed (see section 2)), c) its relationships with urbanization related factors (albedo, decreasing vegetation and increasing population) for the period 2001–2015 in this study. China was chosen as the study area because of its rapid urbanization in recent decades, large area of approximately 9.6 million km^2 and large variations in climate and altitude (Kuang et al., 2016).

2. Data and methods

2.1. Study area

In this study, the SUHI was studied in 31 municipalities (directly governed by the central government) or provincial capitals (Administrative center of a province) (Fig. 1). The 31 cities were divided into 15 southern cities, 15 northern cities and a plateau city (Lhasa). The Qinling Mountain-Huaihe River Line (at about 33°N) was used as dividing line in the present study for two main reasons: a) it is a traditional North-South dividing line in China, and b) the north of this line is different from the south of this line in terms of climate, tree species, agricultural production and people's living customs (Bi et al., 2007; Shi et al., 2013a, 2013b; Wang et al., 2015b; Yao et al., 2017c). Southern China was mainly characterized by humid climate, which was different from the semi-humid, semi-arid and arid climate in Northern China.

2.2. Data

Urban and nonurban areas were extracted from China's Land Use/Cover Datasets (CLUDs, 30 m spatial resolution, 25 land cover types, in the year 2000, 2005, 2010 and 2015), which were generated from Landsat TM/ETM + and HJ-1A/1B imagery. The dataset is provided by Data Center for Resources and Environmental Sciences, Chinese Academy of Sciences (RESDC) (http://www.resdc.cn). The overall accuracy was over 90% for the 25 land cover types according to previous studies (Kuang et al., 2016; Liu et al., 2010, 2014). More information can be found in Kuang et al. (2016), Liu et al. (2014) and Liu et al. (2010).

LST was derived from the MODIS LST data (MOD11A2, version 6, Terra satellite, monitored at 10:30 a.m. and 10:30 p.m., 8-day composite, 1 km spatial resolution, 2001–2015), the accuracy of the LST data was better than 1 K in 39 of 47 cases according to a previous study (Wan, 2008). We used the MOD11A2 product rather than MYD11A2 product since it has longer time series (MOD11A2: February 2000 to present, MYD11A2: July 2002 to present) (He et al., 2017; Yao et al., 2017c, 2018a; 2018b). Vegetation and albedo information was extracted from MODIS enhanced vegetation index (EVI) data (MOD13A2, version 6, Terra satellite, 16-day composite, 1 km spatial resolution, 2001–2015) and MODIS albedo data (MCD43B3, version 5, combined Terra and Aqua satellites, 8-day composite, 1 km spatial resolution, shortwave white sky albedo (WSA), 2001–2015), respectively (Huete et al., 2002; Liang et al., 2002; Peng et al., 2012; Zhou et al., 2014).

Daily climate data from the China Meteorological Administration for the period 2001–2015 was used in this study, including mean air temperature (24-hour mean), total precipitation (24-hour in total), total sunshine duration (24-hour in total) and wind speed (24-hour mean). Weather stations in and around the city were chosen to represent the climate of the city (Fig. 1) (Du et al., 2016; Zhou et al., 2014, 2016a; 2016b). Detailed information about weather stations can be found in Table S1. In addition, non-agriculture population was derived from the statistical yearbook in each city (only available for 23 of the 31 cities). In China, the non-agricultural population refers to the working population engaged in non-agricultural production and the dependent population of their families.

2.3. Extracting urban and rural areas

Twenty-five land cover types of CLUDs were first combined into four major types (urban areas, rural settlements, water bodies and other types) since we only need to distinguish these 4 major land cover types in this study. Next, we generated two types of land cover maps: a) resampled maps, in which CLUDs were resampled to 1 km spatial resolution (matching the MODIS data), and b) proportion maps, where we calculated the proportions of each of the 4 land cover types for each 1 km spatial resolution pixel. Urban areas were then classified into two stationary areas: city center (CC, pixels composed of 100% urban area) and the whole urban area (WUA, total urban area of the four resampled maps) (Fig. 2). In addition, we generated a 20–25 km buffer based on the WUA (Yao et al., 2017b, 2017c; Zhou et al., 2016c), excluding the pixels with a) proportions of urban area plus rural settlements higher than 5% (Imhoff et al., 2010; Zhou et al., 2016a) and b) proportions of water bodies higher than 0%. The resultant areas were then defined as rural areas in this study. The rural areas were set far from the urban areas (20–25 km buffer) because previous studies showed that the extent of SUHIs is much larger than the size of the urban area (Han and Xu, 2013; Zhang et al., 2004; Zhou et al., 2015). In this study, we did not exclude the altitude effects, the reasons can be found in supplementary material 1 (Yao et al., 2018a).

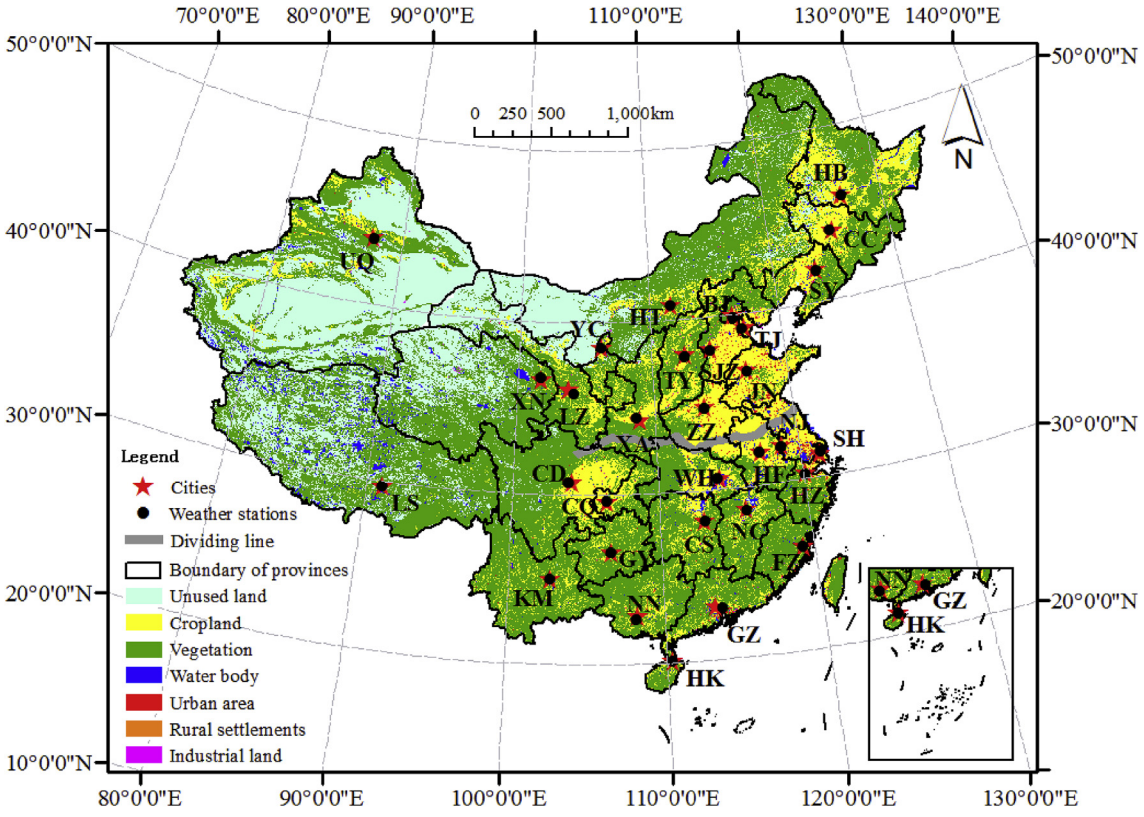

Fig. 1. The locations of the 31 cities and 31 weather stations in this study. 15 northern cities: Harbin (HB), Changchun (CC), Urumqi (UQ), Shenyang (SY), Hohhot (HT), Beijing (BJ), Tianjin (TJ), Yinchuan (YC), Shijiazhuang (SJZ), Taiyuan (TY), Jinan (JN), Xining (XN), Lanzhou (LZ), Zhengzhou (ZZ) and Xi'an (XA). 15 southern cities: Nanjing (NJ), Shanghai (SH), Heifei (HF), Hangzhou (HZ), Wuhan (WH), Chengdu (CD), Chongqing (CQ), Nanchang (NC), Changsha (CS), Fuzhou (FZ), Guiyang (GY), Kunming (KM), Nanning (NN), Guangzhou (GZ) and Haikou (HK). A plateau city was Lhasa (LS). China's Land Use/Cover Datasets in 2010 was used as background map.

2.4. Trends of SUHII

MODIS LST data monitored at 10:30 a.m. and 10:30 p.m. were used to represent daytime and nighttime LST, respectively. Daytime and nighttime LST were then averaged into summer (June to August) and winter (December to February). Thus, this study focused on 4 time periods: summer day (SD), summer night (SN), winter day (WD) and winter night (WN).

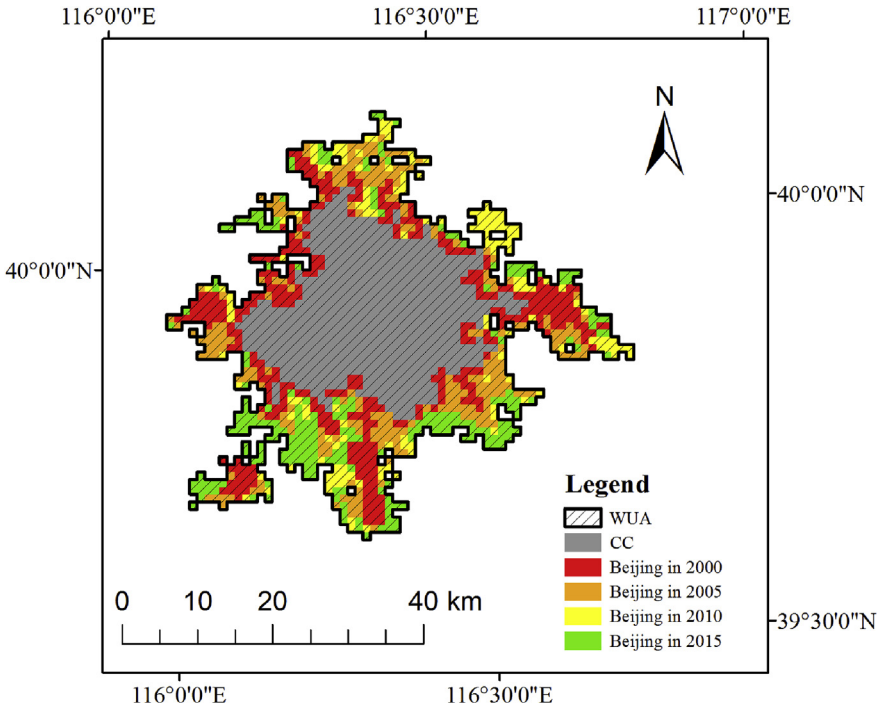

Fig. 2. The schematic diagram of city center (CC) and the whole urban area (WUA). The background maps were the urban area of CLUDs in 2000 (red), 2005 (orange), 2010 (yellow), 2015 (green) in BJ. (For interpretation of the references to colour in this figure legend, the reader is referred to the Web version of this article.)

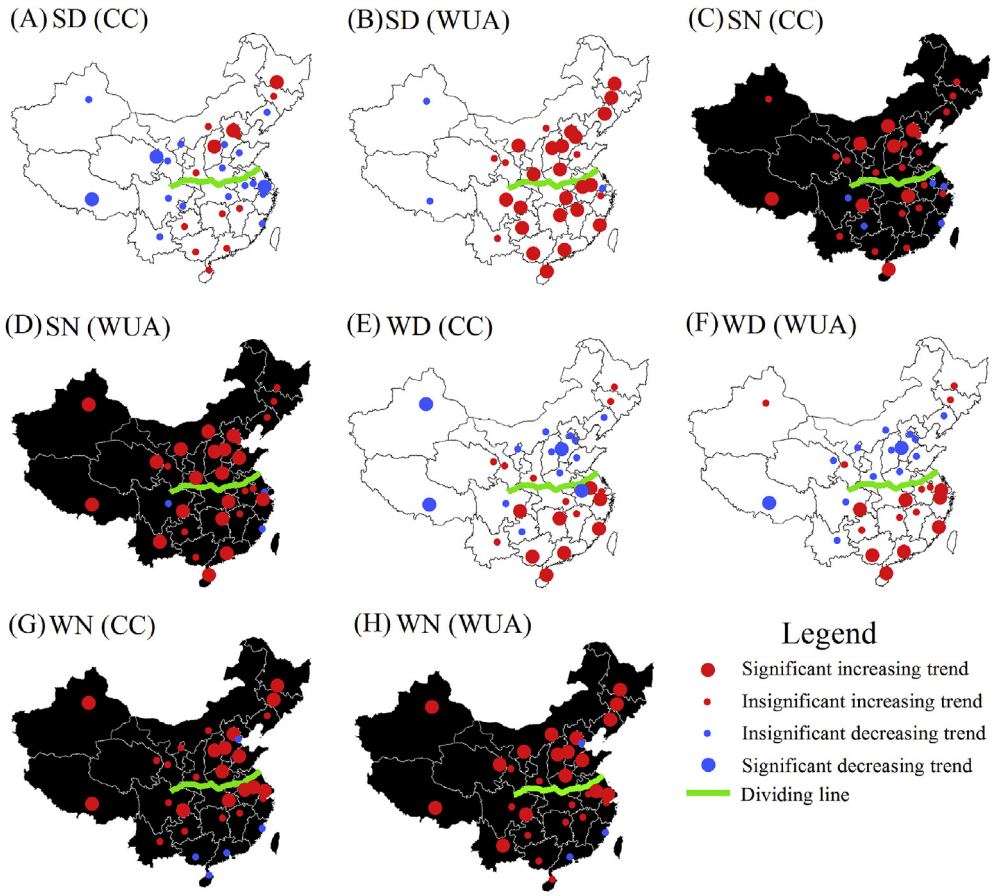

Fig. 3. The temporal trends of surface urban heat island intensity (SUHII) in China for the period 2001–2015. SD: summer day, SN: summer night, WD: winter day, WN: winter night.

The SUHII was calculated using Equations (1) and (2) (Yao et al., 2017a; Zhou et al., 2015):

$$\Delta LST1 = LST_{CC} - LST_{rural} \quad (1)$$

$$\Delta LST2 = LST_{WUA} - LST_{rural} \quad (2)$$

where LST_{CC}, LST_{WUA} and the LST_{rural} are the LST in CC, WUA and rural areas, respectively. ΔLST1 and ΔLST2 are the SUHII in CC and WUA, respectively. The interannual variations in SUHII in each city were analyzed using linear regression analyses (section 3.1).

2.5. Drivers for SUHII variations

Two variables from remote sensing (EVI and WSA) and four variables from weather stations (mean air temperature, total precipitation, total sunshine duration and average wind speed) were also averaged into summer and winter. For non-agriculture population, we hypothesized that it remained constant for the entire year. We also calculated the ΔEVI and the ΔWSA using the same methods as in Equations (1) and (2). Pearson's correlation analyses were performed between SUHII and five climate variables (mean air temperature, background LST (LST in rural areas), total precipitation, total sunshine duration and average wind speed, section 3.2) and three urbanization related variables (non-agriculture population, ΔEVI and ΔWSA, section 3.3) in each city across years, which was different from previous studies across cities (Du et al., 2016; Peng et al., 2012; Wang et al., 2015b; Zhou et al., 2014, 2016b). The correlation analyses across years in this study were compared to the results of correlation analyses across cities in previous studies (section 4.2, 4.3 and 4.4). To further analyze the relationships between urbanization and SUHII, we also conducted Pearson's correlation analyses between the slope of SUHII and the slope of ΔEVI and the slope of non-agriculture population across cities (section 3.4).

2.6. Certain important things

It is important to note the following:

(1) Previous studies showed that the interannual variations of SUHII in urbanized area were dominated by urbanization and nearly invariant with climate variability (Yao et al., 2017c; Zhou et al., 2016a). Consequently, we only performed correlation analyses between SUHII and climate in CC.
(2) Since most of the weather stations in China are located in urban area (Wang et al., 2015a), the mean air temperature was affected by UHI, we also used the background LST to reflect the climate.
(3) MODIS albedo data contain a great number of gaps. Therefore, correlation analyses were conducted if a) the proportion of an available pixel was equal to or higher than 80% in the extent of CC or WUA or rural area (Hu et al., 2016; Weng and Fu, 2014), and b) the proportion of the years that met requirement a) was equal to or higher than 80% (12 years).

2.7. Limitations and uncertainties

Uncertainties exist in this study. Firstly, the time period was relatively short (2001–2015), which may be an important reason for the non-significant correlations between SUHII and climate in the majority of the cities (in section 3.2). The absolute values of the correlation coefficients between SUHII and climate factors in certain cities were higher than 0.45 but were statistically non-significant ($p > 0.05$). Secondly, the method for revealing the relationship between SUHII and

driving factors in this study was Pearson's correlation analysis, which is relatively simple and unreliable. The form of relationship curve may not necessarily be linear. For example, Zhou et al. (2016b) found a quadratic relationship between mean annual SUHII and mean annual total precipitation across Chinese cities, suggesting that the effects of local background climate on SUHII might have a threshold (Zhou et al., 2016b). However, it was difficult to explore the actual relationships for each variable, city and time period. Thirdly, certain continuous data at regional scale was very scarce up till now. Therefore, the relationships between interannual variations of SUHII and some important factors have not been investigated, including urban size (Clinton and Gong, 2013) and urban development intensity (Zhou et al., 2016a). Fourthly, we divided 31 cities into southern cities and northern cities, however, the climate varied greatly in northern cities (semi-humid, semi-arid and arid). Overall, detailed study in a single city with longer study period will be conducted in future.

3. Results

3.1. The interannual variations of SUHII in 31 cities in China

The temporal SUHII trends for the period 2001–2015 are shown in Fig. 3. For the WUA, the SUHII increased in most of the cities on SDs (28 of the 31 cities), SNs (28 of the 31 cities) and WNs (29 of the 31 cities). Significant increasing trends ($p < 0.05$) of SUHII were observed in 22, 18 and 17 of the 31 cities for SDs, SNs and WNs, respectively (Fig. 3). For the 31 cities averaged, the SUHII increased significantly on SDs, SNs and WNs, respectively (Table 1). Additionally, significant increasing trends were observed in fewer cities in CC than in the WUA (8 and 14 of the 31 cities for SNs and WNs, respectively), especially on SDs (only 3 of the 31 cities). In addition, the significant increasing trends of SUHII on WDs were all found in southern cities, while the SUHII decreased in most of the northern cities (Fig. 3). Finally, the number of cities with significant increasing trends of nighttime SUHII was higher in Northern China than in Southern China (Fig. 3). The increasing rates of nighttime SUHII were higher in northern cities than in southern cities (Table 1).

3.2. The relationships between interannual variations of SUHII and climate variability

The influences of climate factors on interannual variations in SUHII depended on time periods and geographical positions (Table 2). On SDs and WDs, positive correlations between SUHII and total precipitation were observed in most of the northern cities, Significant positive correlations between SUHII and precipitation on SDs were mainly observed in arid and semi-arid northwestern cities (e.g. Urumqi, Lanzhou, Yinchuan, Hohhot), while insignificant positive correlations were mainly found in semi-humid northeast cities (explanations in section 4.2.1) (Zhou et al., 2016b). Comparatively, negative correlations between nighttime SUHII and total precipitation were found in most of the cities in China (Table 2). Significant negative correlations were found in 6 of the 15 southern cities on WNs (explanations in section 4.2.3).

The SUHII on SDs and WDs was generally invariant with total sunshine duration, with significant correlations found in few cities (Table 2) (explanations in section 4.2.1). In contrast, positive correlations between SUHII and total sunshine duration were found in most of the cities in China on SNs and WNs (Table 2). Nearly half of the cities showed significant positive correlations on SNs in Northern China (7 of the 15 cities) and on WNs in Southern China (8 of the 15 cities) (explanations in section 4.2.3).

The SUHII on SDs and WDs was negatively correlated with mean air temperature in most of the northern cities, and significant negative correlations were found in 6 of the 15 cities on WDs (Table 2) (explanations in section 4.2.1 and 4.2.2). Comparatively, the nighttime SUHII was positively correlated with the mean air temperature for most of the cities in summer for the entirety of China (26 of the 31 cities) and in winter in Southern China (12 of the 15 cities) (explanations in section 4.2.3).

The SUHII was negatively correlated with the background LST in all 15 cities in Northern China on both SDs and WDs, and significant negative correlations were observed in approximately two-thirds of the cities (11 and 10 of the 15 cities for summer and winter, respectively) (explanations in section 4.2.1 and 4.2.2). The background LST has less impact on daytime SUHII for southern cities and on nighttime SUHII for all of China, the significant correlations were found in few cities (Table 2).

The interannual variations of SUHII were almost invariant with average wind speed (Table 2). The number of cities with positive correlations between SUHII and average wind speed was almost equal to the number of the cities with negative correlations. In addition, significant relations between SUHII and average wind speed were only found in few cities. Finally, coastal cities did not show obvious different correlations between SUHII and average wind speed than inland cities, plain cities did not show obvious different correlations between SUHII and average wind speed than mountains cities (data not shown).

The trends of climate drivers were shown in Table S2. The mean air

Table 2
The relationships between SUHII and climate factors in China. The number of the cities with positive and negative correlations was showed in left and right, respectively. The numbers of the cities with significant correlations was showed in the brackets.

Region	SD	SN	WD	WN
SUHII & total precipitation				
Northern China	14(5), 1(0)	3(0), 12(1)	12(0), 3(0)	3(0), 12(3)
Southern China	8(0), 7(0)	3(0), 12(2)	8(0), 7(0)	2(0), 13(6)
Entire China	23(5), 8(0)	6(0), 25(3)	21(0), 10(0)	6(1), 25(9)
SUHII & total sunshine duration				
Northern China	5(0), 10(2)	10(7), 5(0)	4(0), 11(2)	10(1), 5(1)
Southern China	8(0), 7(0)	11(0), 4(0)	8(1), 7(2)	13(8), 2(0)
Entire China	13(0), 18(3)	22(8), 9(0)	12(1), 19(5)	24(9), 7(1)
SUHII & mean air temperature				
Northern China	3(0), 12(2)	13(2), 2(0)	1(0), 14(6)	5(0), 10(4)
Southern China	6(0), 9(0)	12(3), 3(1)	6(1), 9(2)	12(1), 3(1)
Entire China	9(0), 22(3)	26(6), 5(1)	7(1), 24(8)	17(1), 14(6)
SUHII & background LST				
Northern China	0(0), 15(11)	8(0), 7(0)	0(0), 15(10)	4(0), 11(6)
Southern China	4(0), 11(3)	9(0), 6(0)	3(0), 12(3)	8(1), 7(0)
Entire China	4(0), 27(15)	18(1), 13(0)	3(0), 28(14)	12(1), 19(6)
SUHII & average wind speed				
Northern China	8(1), 7(2)	4(0), 11(1)	6(1), 9(0)	5(0), 10(5)
Southern China	8(1), 7(0)	12(1), 3(0)	8(0), 7(3)	10(1), 5(2)
Entire China	16(2), 15(2)	17(1), 14(1)	14(1), 17(3)	16(1), 15(7)

Table 1
The temporal trends of surface urban heat island intensity (SUHII) in China averaged for southern cities, northern cities and the entire China. Significance levels: * $p < 0.05$, ** $p < 0.01$. SD: summer day, SN: summer night, WD: winter day, WN: winter night. CC: city center, WUA: whole urban area. Unit: °C/year.

Region	SD (CC)	SD (WUA)	SN (CC)	SN (WUA)	WD (CC)	WD (WUA)	WN (CC)	WN (WUA)
Northern China	0.024	0.094**	0.034**	0.051**	−0.034	−0.027	0.064**	0.064**
Southern China	−0.006	0.122**	0.014	0.028**	0.079**	0.061**	0.035	0.026
Entire China	0.003	0.101**	0.029**	0.042**	0.017	0.010	0.049**	0.044**

Table 3
The relationships between SUHII and urbanization related factors in China. The number of the cities with positive and negative correlations was showed in left and right, respectively. The number of the cities with significant correlations was showed in the brackets.

Region	SD (CC)	SD (WUA)	SN (CC)	SN (WUA)	WD (CC)	WD (WUA)	WN (CC)	WN (WUA)
SUHII & ΔEVI								
Northern China	1(0), 14(10)	0(0), 15(12)	9(1), 6(2)	2(0), 13(7)	13(4), 2(1)	12(5), 3(0)	9(3), 6(3)	9(2), 6(4)
Southern China	4(1), 11(1)	1(1), 14(11)	4(0), 11(2)	2(0), 13(4)	4(0), 11(4)	4(0), 11(4)	6(0), 9(5)	2(0), 13(6)
Entire China	5(1), 26(11)	1(1), 30(23)	14(1), 17(4)	4(0), 27(12)	17(4), 14(5)	17(6), 14(4)	16(3), 15(8)	11(2), 20(10)
SUHII & non-agriculture population								
Northern China	6(1), 4(1)	8(6), 2(0)	10(4), 0(0)	10(7), 0(0)	3(0), 7(0)	3(0), 7(0)	8(4), 2(0)	8(5), 2(0)
Southern China	4(1), 9(1)	12(9), 1(1)	7(3), 6(0)	10(7), 3(0)	7(4), 6(1)	9(3), 4(0)	10(3), 3(0)	11(1), 2(0)
Entire China	10(2), 13(2)	20(15), 3(1)	17(7), 6(0)	20(14), 3(0)	10(4), 13(1)	12(3), 11(0)	18(7), 5(0)	19(6), 4(0)
SUHII & ΔWSA								
Northern China	5(0), 6(2)	6(1), 6(1)	7(1), 4(2)	9(1), 3(1)	0, 6(3)	0, 7(6)	3(1), 3(1)	3(0), 4(1)
Southern China	0, 0	0, 0	0, 0	0, 0	1(0), 0	1(0), 0	0, 1(0)	1(0), 0
Entire China	6(1), 6(2)	7(1), 6(1)	7(1), 5(2)	10(1), 3(1)	2(1), 6(3)	2(0), 7(6)	3(1), 5(2)	4(0), 5(2)

temperature, total sunshine duration, total precipitation and background LST did not change significantly in most cities for the period 2001–2015, while the average wind speed changed significantly in over half of the 31 cities.

3.3. The relationships between interannual variations of SUHII and urbanization

Decreasing △EVI was an important reason for the increasing SUHII in summer (Table 3). The SUHII was negatively correlated with the △EVI in most of the cities in the WUA in summer (30 and 27 of the 31 cities for SDs and SNs, respectively). Significant correlations were observed in over two-thirds and one-third of the cities in the WUA for SDs and SNs, respectively (Table 3). In addition, the △EVI has less impact on SUHII in winter (Table 3) (explanations in section 4.3.1).

The SUHII was positively correlated with the non-agriculture population for most of the cities in the WUA on SDs, SNs and WNs. Significant positive correlations were observed in over half of the cities in the WUA on SDs and SNs (Table 3). In addition, the non-agriculture population had less impact on SUHII in CC as the number of cities with positive or significant positive correlations was less in CC than in the WUA on SDs and SNs (Table 3) (explanations in section 4.3.1).

Surprisingly, significant correlations between SUHII and △WSA were observed in few cities on SDs, SNs and WNs (Table 3). Meanwhile, the SUHII was significantly and negatively correlated with the △WSA in some northern cities on WDs. The relationships between interannual variation of SUHII and △WSA were completely different from our previous understanding that the △WSA was a major driver for nighttime SUHII and that daytime SUHII was generally invariant with △WSA (explanations in section 4.3.1).

The trends of urbanization related drivers were shown in Table S3. The △EVI in WUA decreased significantly in most cities in summer, while the non-agriculture population increased significantly in all of the 23 cities. In addition, the △WSA did not decrease significantly although urbanization occurred in those cities.

3.4. Correlation analyses between linear changing rate of SUHII and drivers across cities

The correlations across cities showed that cities with greater decreasing rates of △EVI showed higher increasing rates of SUHII on SDs and WDs (Table 4). Comparatively, the slopes of △EVI and nighttime SUHII were almost irrelevant. In addition, the slope of SUHII was positively correlated with the slope of non-agriculture population in most cases, however, no significant correlations were observed. This pattern suggested that the cities with higher increasing rates of non-agriculture population will not necessarily show higher increasing rates of SUHII (explanations in section 4.3.2).

4. Discussion

4.1. The temporal trends of SUHII

The SUHII changed dramatically in China, over half of the cities in the WUA showed significant increasing trends on SDs, SNs and WNs (Fig. 3). The number of cities with significant increasing trends of SUHII in this study was similar to Yao et al. (2017c) but larger than Zhou et al. (2016a), the reason may be attributed to the study period (this study: 2001–2015; Yao et al. (2017c): 2001–2015; Zhou et al. (2016a): 2003–2012). In addition, the number of cities with significant increasing trends of SUHII in the WUA was more than in CC, which was similar to the findings reported by Zhou et al. (2016a) and Yao et al. (2017c), as urbanization primarily occurred in urban areas other than CC.

The temporal trends of SUHII on WDs averaged for 15 southern cities and 15 northern cities increased significantly and decreased insignificantly, respectively (Table 1). These can be attributed to different vegetation species. Some southern cities are surrounded by evergreen forest, in contrast to the deciduous forests of the northern cities (Zhou et al., 2014). Evergreen forest is green throughout the year, while the deciduous forest browns in winter. Thus, deciduous forest is always brown in winter before and after urbanization, while evergreen forest in winter is green before urbanization and brown after urbanization. Thus increased urbanization can decrease vegetation and increase SUHII in southern cities (Yao et al., 2017a; Zhou et al., 2014). The insignificant decreasing trend of SUHII on WDs in Northern China may be attributed to the increasingly serious air pollution. Serious air pollution may decrease the daytime SUHII through reducing the solar radiation and increase the nighttime SUHII through increasing the longwave radiation (Cao et al., 2016; Wu et al., 2017).

The increasing trends of SUHII on SNs and WNs averaged for northern cities were much higher than southern cities (Table 1). Southern cities are much more humid than northern cities and the soil moisture is much higher in southern cities than in northern cities (Zhou et al., 2014). Therefore, the SUHII on SNs and WNs in northern cities is much higher than in southern cities since the soil moisture can influence the changing rate of LST (Winguth and Kelp, 2013; Zhou et al., 2014). As rapid urbanization, drier soil (northern cities) transformed into urban roads and buildings, which can lead to higher increasing trends of nighttime SUHII compared to the wetter soil (southern cities) (Yao et al., 2017c).

4.2. The relationships between SUHII and climate variability in China

The correlation analyses between SUHII and associated drivers can be conducted across space and time. Most of the previous studies analyzed the relationships between SUHII and its drivers across cities (Clinton and Gong, 2013; Du et al., 2016; Imhoff et al., 2010; Peng

Table 4
The Pearson's correlations between the slope of ΔEVI or the slope of non-agriculture population and the slope of SUHII.

	SD (CC)	SD (WUA)	SN (CC)	SN (WUA)	WD (CC)	WD (WUA)	WN (CC)	WN (WUA)
The slope of SUHII and the slope of △EVI								
Correlation coefficient	−0.699	−0.683	−0.101	−0.225	−0.586	−0.503	0.331	0.418
Significant level	$p < 0.01$	$p < 0.01$	$p = 0.588$	$p = 0.224$	$p < 0.01$	$p < 0.01$	$p = 0.069$	$p < 0.05$
R square	0.488	0.466	0.010	0.051	0.343	0.253	0.110	0.175
The slope of SUHII and the slope of non-agriculture population								
Correlation coefficient	−0.083	0.027	0.113	0.105	0.172	0.140	0.077	0.046
Significant level	0.707	0.901	0.608	0.633	0.433	0.523	0.726	0.837
R square	0.007	0.001	0.013	0.011	0.030	0.020	0.006	0.002

et al., 2012; Wang et al., 2015b; Zhou et al., 2014, 2016b). Few studies have analyzed the relationships across time. In this study, we performed correlation analyses across years, and a series of new and different findings were revealed.

4.2.1. The influences of total precipitation, temperature and total sunshine duration on SUHII on SDs

In this study, the SUHII on SDs was positively correlated with total precipitation in most of the cities in Northern China, especially in Northwest China. However, Du et al. (2016) and Zhou et al. (2014) found negative correlations between SUHII and precipitation on SDs in Yangtze River Delta (China) and China, respectively. In addition, the SUHII on SDs was negatively related to mean air temperature and background LST in most of the cities in Northern China (Table 2). These results were completely different from the correlation analyses across cities in Du et al. (2016) and Zhou et al. (2016b), which showed significant positive correlations between SUHII and mean air temperature. But these were similar to Yao et al. (2017c), which also showed negative correlations between SUHII and background LST across years in most cities in northern China. The present findings were also different from the phenomenon that a UHI can be enhanced by heatwaves (Li and Bou-Zeid, 2013; Ramamurthy and Bou-Zeid, 2017). Furthermore, the total sunshine duration was insignificantly related to the SUHII on SDs in most of the cities.

In this study, the influences of total precipitation and temperature on SUHII on SDs may be explained by vegetation growth and soil moisture. The soil in rural areas has much higher water retention ability than urban roads or buildings (Du et al., 2016), but low precipitation and high temperature on SDs can decrease the soil moisture in rural areas (Du et al., 2016; Winguth and Kelp, 2013). Therefore, the LST will quickly increase in rural areas during the daytime and then decrease the SUHII. In addition, low soil moisture have negative impacts on vegetation, especially in certain arid and semi-arid northwest cities (Piao, 2003). These conditions can decrease the EVI in rural areas and increase the △EVI (EVI in urban minus rural), which finally decreases the SUHII (Table S4 and S5). Thus, low precipitation and high temperature could increase the LST in urban and rural simultaneously, but the increase in LST in rural was higher than urban, thus increasing the SUHII. Furthermore, long sunshine duration can also decrease the soil moisture and has negative impacts on vegetation in arid region, increase the LST in rural area (Table S6). But long sunshine duration can increase the LST in urban area simultaneously. That may be the reason for the insignificant correlations between SUHII and total sunshine duration in most of the cities on SDs. Finally, previous studies analyzed the relationships between UHI and heatwaves on different dates in the same year and showed that the UHI can be enhanced by heatwaves (Li and Bou-Zeid, 2013; Ramamurthy and Bou-Zeid, 2017), but over a short time period, vegetation activity will not change notably (Yao et al., 2017c).

4.2.2. The influences of ice and snow on SUHII on WDs

In this study, the SUHII on WDs was negatively correlated with temperature in northern cities. These were different from insignificant correlation or significant positive correlation across cities in previous studies (Peng et al., 2012; Zhou et al., 2014; Du et al., 2016).

In cold years, low temperatures increase the snow and ice in rural areas, increasing the albedo due to the high albedo of snow and ice. The higher albedo reflects more solar radiation to the sky and further decreases the LST (Xu et al., 2017). Comparatively, snow and ice on urban roads and buildings are often removed by humans, decreasing the △WSA (urban WSA minus rural) and finally increasing the SUHII (Table 3 and Table S7). This phenomenon was more evident in Northern China since the snow and ice cover usually happened in northern cities (Table 2).

4.2.3. The influences of temperature, total precipitation and total sunshine duration on SUHII on SNs and WNs

In this study, the SUHII on SNs and WNs was negatively correlated with total precipitation in most cities in China, these were similar to the correlation analyses across cities in previous studies (Du et al., 2016; Zhou et al., 2014; Peng et al., 2012). In addition, the nighttime SUHII was significantly and positively correlated with total sunshine duration in approximately half of the cities in Northern China in summer and in Southern China in winter, these were similar to the correlation analyses across time in Zhou et al. (2011). Furthermore, the SUHII was positively correlated with mean air temperature on SNs in most of the cities. These were different from Peng et al. (2012) and Zhou et al. (2014), which showed negative correlation between SUHII and mean air temperature across cities.

The influences of total precipitation, total sunshine duration and mean air temperature on SUHII on SNs and WNs may also be explained by soil moisture. The increasing precipitation can increase soil moisture, while decreasing sunshine duration and mean air temperature can reduce the evaporation of soil moisture. These can lower the rate of decrease of LST in rural areas during nighttime, and finally decrease the SUHII. In addition, these impacts were seemingly less evident in Northern China in winter, probably because of the snow and ice, and in Southern China, in summer likely due to the excessive precipitation and saturated soil moisture.

4.3. The relationships between SUHII and urbanization in China

4.3.1. The correlation analyses between SUHII and associated drivers across years

In this study, the SUHII was negatively correlated with △EVI on SDs in most cities in China, which suggested that decreasing vegetation may be a major factor contributing to the SUHII, these were the same as previous studies and can be attributed to the cooling effect of vegetation (Peng et al., 2012; Zhou et al., 2014). In addition, the decreasing △EVI may be an important reason for the increased SUHII on SNs for the whole China and on WDs for southern cities (Table 3). These findings were similar to Yao et al. (2017c), which found negative correlations between SUHII and △EVI across years in most cities in China. The negative correlations on SNs may be attributed to the excess heat stored during daytime due to urbanization (Quan et al., 2016; Tiangco et al., 2008; Doick et al., 2014), while on WDs possibly due to the

evergreen forests around these cities.

In the present study, increased population may be an important reason for the increased SUHII (Table 3). This finding was different from the spatial analyses of Du et al. (2016) and Peng et al. (2012) but consistent with Hung et al. (2006). In this research, the increasing population due to the urbanization can decrease the vegetation, increase roads, buildings and energy consumption, and then increase the SUHII indirectly.

In this study, the SUHII on SNs and WNs was insignificantly correlated with the albedo in most of the cities from temporal perspectives. These were different from the spatial perspectives in previous studies (Peng et al., 2012; Wang et al., 2015b; Zhou et al., 2014). In the present study, the △WSA did not decrease significantly although rapid urbanization occurred in those cities (Table S3). Thus, other factors, such as total precipitation and total sunshine duration, may play more important roles in SUHII on SNs and WNs. Zhou et al. (2014) showed that the △WSA was lower in Northern China than in Southern China because of the different vegetation types, which was a major factor for the higher nighttime SUHII in Northern China than in Southern China. However, as vegetation types did not change in the same location across years, the △WSA may also be stable. These factors may be the reasons for the non-significant correlations between SUHII and △WSA across years observed in the present study.

4.3.2. The correlation analyses between linear changing rate of SUHII and associated drivers across cities

Correlation analyses across cities showed that cities with greater decreasing rates of △EVI may have higher increasing rates of SUHII on SDs and WDs, but this is not the case for the SUHII on SNs and WNs (Table 4). These were different from Yao et al. (2017a). Vegetation can decrease temperature directly by evapotranspiration during daytime, thus, the slope of SUHII was tightly correlated to the slope of △EVI. However, the decreasing △EVI may increase nighttime SUHII indirectly through increasing the amount of heat during daytime (Quan et al., 2016; Tiangco et al., 2008; Doick et al., 2014). Other factors that are tightly linked to nighttime SUHII were different in various cities, for example, soil moisture and anthropogenic heat release (Zhou et al., 2014). Therefore, on SNs and WNs, the correlations between the slope of SUHII and the slope of △EVI across cities were non-significant.

Interestingly, increased non-agriculture population may be an important reason for the increased SUHII, but cities with higher increasing rates of non-agriculture population might not have higher increasing rates of SUHII (Table 4). Increasing non-agriculture population may increase the SUHII but in ways that are also indirect: through increasing urban roads, buildings and energy consumption. However, the number of increased roads or buildings and the increased energy consumption may not be correlated with the increased non-agriculture population across cities. These factors led to the non-significant correlations between the slope of SUHII and the slope of non-agriculture population.

4.4. Correlation analyses across space and time

In this study, some drivers might not change significantly in the same place across years, especially when averaged into season. This factor may lead to insignificant correlations between SUHII and some drivers, subsequently ignoring the importance of these drivers, for example albedo. The correlation analyses across cities conducted in different regions can lead to different results according to previous studies. Therefore, limitations existed in the correlation analyses across both space and time. For comprehensively understanding the relationships between SUHII and drivers, it is necessary to analyze the relationships across both space and time. However, if we would like to accurately find the associated drivers and mitigation strategies of SUHII in single city, it is better to analyze the relationships between SUHII and drivers across years.

The comparisons between correlation analyses across cities (in previous studies) and years (this study) can improve our understanding of the relationships between SUHII and related drivers. It suggested that the drivers of spatial variations in SUHII may not be the same as the drivers of interannual variations in SUHII. In addition, previous studies only analyzed the relationships between interannual variations in SUHII and several factors (vegetation, air temperature, precipitation and anthropogenic heat release) (Zhou et al., 2016a; Yao et al., 2017a, 2017c). This study showed that total sunshine duration, population and albedo may also influence the interannual variations in SUHII. Interestingly, these three factors linked with the SUHII in different time periods.

5. Conclusions

Interannual variations in SUHII and possible drivers were systematically analyzed in this study. Significant increasing trends of SUHII in the WUA were observed in 22, 18, 8 and 17 of the 31 cities on SDs, SNs, WDs and WNs, respectively. The SUHII in CC increased significantly in 3, 8, 8 and 14 of the 31 cities on SDs, SNs, WDs and WNs, respectively.

Correlation analyses between SUHII and climate or urbanization related variables were performed across years, and we found that in many cases, the results were completely different from those of the spatial analyses. For climate factors, the SUHII on SNs and WNs in most of the cities was negatively and positively correlated with the total precipitation and total sunshine duration, respectively. Total precipitation was positively correlated with the SUHII in most of the northern cities on SDs. The SUHII on SDs and WDs was negatively correlated with mean air temperature and background LST in most of the cities. Average wind speed had little effect on SUHII.

For urbanization related factors, increased non-agriculture population and decreasing vegetation were important reasons for increased SUHII, while albedo only influenced the SUHII on WDs. Cities with greater decreasing rates of ΔEVI showed higher increasing rates of daytime SUHII instead of nighttime SUHII. The higher increasing rates of non-agriculture population did not lead to higher increasing rates of SUHII.

The above findings provide a reference for studying the interannual variations of SUHI and a better understanding of the relationships between SUHIs and their driving forces. The increasing trend of SUHII may not stop in China as continuous urbanization. Therefore, effective measures should be taken to mitigate the SUHII.

Acknowledgments

This work was financially supported by the National Natural Science Foundation of China (No.41601044), the Special Fund for Basic Scientific Research of Central Colleges, China University of Geosciences, Wuhan (No.CUG15063 and CUGL170401), and the Natural Science Foundation for Distinguished Young Scholars of Hubei Province of China (No. 2016CFA051).

Appendix A. Supplementary data

Supplementary data related to this article can be found at http://dx.doi.org/10.1016/j.jenvman.2018.05.024.

References

Bi, X., Feng, Y., Wu, J., Wang, Y., Zhu, T., 2007. Source apportionment of PM10 in six cities of northern China. Atmos. Environ. 41, 903–912.
Cao, C., Lee, X., Liu, S., Schultz, N., Xiao, W., Zhang, M., Zhao, L., 2016. Urban heat islands in China enhanced by haze pollution. Nat. Commun. 7, 12509.
Clinton, N., Gong, P., 2013. MODIS detected surface urban heat islands and sinks: global locations and controls. Remote Sens. Environ. 134, 294–304.
Curriero, F., Heiner, K., Samet, J., Zeger, S., Strug, L., Patz, J., 2002. Temperature and mortality in 11 cities of the eastern United States. Am. J. Epidemiol. 155, 80–87.
Doick, K.J., Peace, A., Hutchings, T.R., 2014. The role of one large greenspace in mitigating London's nocturnal urban heat island. Sci. Total Environ. 493, 662–671.

Du, H., Wang, D., Wang, Y., Zhao, X., Qin, F., Jiang, H., Cai, Y., 2016. Influences of land cover types, meteorological conditions, anthropogenic heat and urban area on surface urban heat island in the Yangtze River Delta urban agglomeration. Sci. Total Environ. 571, 461–470.
Giorgio, G.A., Ragosta, M., Telesca, V., 2017. Climate variability and industrial-suburban heat environment in a mediterranean area. Sustainability 9, 775.
Grimm, N.B., Faeth, S.H., Golubiewski, N.E., Redman, C.L., Wu, J., Bai, X., et al., 2008. Global change and the ecology of cities. Science 319, 756–760.
Han, G., Xu, J., 2013. Land surface phenology and land surface temperature changes along an urban-rural gradient in Yangtze River Delta, China. Environ. Manag. 52, 234–249.
He, C., Gao, B., Huang, Q., Ma, Q., Dou, Y., 2017. Environmental degradation in the urban areas of China: evidence from multi-source remote sensing data. Remote Sens. Environ. 193, 65–75.
Hu, L., Monaghan, A., Voogt, J.A., Barlage, M., 2016. A first satellite-based observational assessment of urban thermal anisotropy. Remote Sens. Environ. 181, 111–121.
Hua, L., Ma, Z., Guo, W., 2008. The impact of urbanization on air temperature across China. Theor. Appl. Climatol. 93, 179–194.
Huete, A., Didan, K., Miura, T., Rodriguez, E.P., Gao, X., Ferreira, L.G., 2002. Overview of the radiometric and biophysical performance of the MODIS vegetation indices. Remote Sens. Environ. 83, 195–213.
Hung, T., Uchihama, D., Ochi, S., Yasuoka, Y., 2006. Assessment with satellite data of the urban heat island effects in Asian mega cities. Int. J. Appl. Earth. Obs. 8, 34–48.
Imhoff, M.L., Bounoua, L., DeFries, R., Lawrence, W.T., Stutzer, D., Tucker, C.J., Ricketts, T., 2004. The consequences of urban land transformation on net primary productivity in the United States. Remote Sens. Environ. 89, 434–443.
Imhoff, M.L., Zhang, P., Wolfe, R.E., Bounoua, L., 2010. Remote sensing of the urban heat island effect across biomes in the continental USA. Remote Sens. Environ. 114, 504–513.
Kuang, W., Liu, J., Dong, J., Chi, W., Zhang, C., 2016. The rapid and massive urban and industrial land expansions in China between 1990 and 2010: a CLUD-based analysis of their trajectories, patterns, and drivers. Landsc. Urban Plan. 145, 21–33.
Li, D., Bou-Zeid, E., 2013. Synergistic interactions between urban heat islands and heat waves: the impact in cities is larger than the sum of its parts*. J. Appl. Meteorol. Clim. 52, 2051–2064.
Liang, S., Fang, H., Chen, M., Shuey, C.J., Walthall, C., Daughtry, C., Morisette, J., Schaaf, C., Strahler, A., 2002. Validating MODIS land surface reflectance and albedo products: methods and preliminary results. Remote Sens. Environ. 83, 149–162.
Liu, J., Kuang, W., Zhang, Z., Xu, X., Qin, Y., Ning, J., Zhou, W., Zhang, S., Li, R., Yan, C., Wu, S., Shi, X., Jiang, N., Yu, D., Pan, X., Chi, W., 2014. Spatiotemporal characteristics, patterns, and causes of land-use changes in China since the late 1980s. J. Geogr. Sci. 24, 195–210.
Liu, J., Zhang, Z., Xu, X., Kuang, W., Zhou, W., Zhang, S., Li, R., Yan, C., Yu, D., Wu, S., Jiang, N., 2010. Spatial patterns and driving forces of land use change in China during the early 21st century. J. Geogr. Sci. 20, 483–494.
Liu, L., Zhang, Y., 2011. Urban heat island analysis using the Landsat TM data and ASTER data: a case study in Hong Kong. Rem. Sens. 3, 1535–1552.
Peng, S., Piao, S., Ciais, P., Friedlingstein, P., Ottle, C., Breon, F.M., Nan, H., Zhou, L., Myneni, R.B., 2012. Surface urban heat island across 419 global big cities. Environ. Sci. Technol. 46, 696–703.
Piao, S., 2003. Interannual variations of monthly and seasonal normalized difference vegetation index (NDVI) in China from 1982 to 1999. J. Geophys. Res. 108.
Quan, J., Zhan, W., Chen, Y., Wang, M., Wang, J., 2016. Time series decomposition of remotely sensed land surface temperature and investigation of trends and seasonal variations in surface urban heat islands. J. Geophys. Res. Atmos. 121, 2638–2657.
Ramamurthy, P., Bou-Zeid, E., 2017. Heatwaves and urban heat islands: a comparative analysis of multiple cities. J. Geophys. Res. Atmos. 122, 168–178.
Shi, Y., Ge, Y., Chang, J., Shao, H., Tang, Y., 2013a. Garden waste biomass for renewable and sustainable energy production in China: potential, challenges and development. Renew. Sustain. Energy Rev. 22, 432–437.
Shi, P., Ma, X., Hou, Y., Li, Q., Zhang, Z., Qu, S., Chen, C., Cai, T., Fang, X., 2013b. Effects of land-use and climate change on hydrological processes in the upstream of Huai river, China. Water Resour. Manag. 27, 1263–1278.
Tao, M., Chen, L., Wang, Z., Wang, J., Tao, J., Wang, X., 2016. Did the widespread haze pollution over China increase during the last decade? A satellite view from space. Environ. Res. Lett. 11, 054019.
Tiangco, M., Lagmay, A.M.F., Argete, J., 2008. ASTER-based study of the night-time urban heat island effect in Metro Manila. Int. J. Rem. Sens. 29, 2799–2818.
United Nations, 2014. World Urbanization Prospects: the 2013 Revision.
Voogt, J.A., Oke, T.R., 2003. Thermal remote sensing of urban climates. Remote Sens. Environ. 86, 370–384.
Wan, Z., 2008. New refinements and validation of the MODIS Land-Surface Temperature/Emissivity products. Remote Sens. Environ. 112, 59–74.
Wang, F., Ge, Q., Wang, S., Li, Q., Jones, P.D., 2015a. A new estimation of Urbanization's contribution to the warming trend in China. J. Clim. 28, 8923–8938.
Wang, H., Zhang, Y., Tsou, J.Y., Li, Y., 2017. Surface urban heat island analysis of Shanghai (China) based on the change of land use and land cover. Sustainability 9, 1538.
Wang, J., Huang, B., Fu, D., Atkinson, P., 2015b. Spatiotemporal variation in surface urban heat island intensity and associated determinants across major Chinese cities. Rem. Sens. 7, 3670–3689.
Wang, W., Zeng, Z.M., Karl, T.R., 1990. Urban heat island in China. Geophys. Res. Lett. 17 (22), 2377–2380.
Weng, Q., Fu, P., 2014. Modeling annual parameters of clear-sky land surface temperature variations and evaluating the impact of cloud cover using time series of Landsat TIR data. Remote Sens. Environ. 140, 267–278.
Winguth, A.M.E., Kelp, B., 2013. The urban heat island of the north-Central Texas region and its relation to the 2011 severe Texas drought. J. Appl. Meteorol. Clim 52, 2418–2433.
Wu, H., Wang, T., Riemer, N., Chen, P., Li, M., Li, S., 2017. Urban heat island impacted by fine particles in Nanjing, China. Sci. Rep. 7, 11422.
Xian, G., Crane, M., 2006. An analysis of urban thermal characteristics and associated land cover in Tampa Bay and Las Vegas using Landsat satellite data. Remote Sens. Environ. 104, 147–156.
Xu, L., Zeng, Z., Yao, Y., Peng, S., Wang, K., Piao, S., 2017. Spatiotemporal variations in the difference between satellite-observed daily maximum land surface temperature and station-based daily maximum near-surface air temperature. J. Geophys. Res. Atmos. 122, 2254–2268.
Yao, R., Wang, L., Gui, X., Zheng, Y., Zhang, H., Huang, X., 2017a. Urbanization effects on vegetation and surface urban heat islands in China's Yangtze River basin. Rem. Sens. 9, 540.
Yao, R., Wang, L., Huang, X., Guo, X., Niu, Z., Liu, H., 2017b. Investigation of urbanization effects on land surface phenology in northeast China during 2001–2015. Rem. Sens. 9, 66.
Yao, R., Wang, L., Huang, X., Niu, Z., Liu, F., Wang, Q., 2017c. Temporal trends of surface urban heat islands and associated determinants in major Chinese cities. Sci. Total Environ. 609, 742–754.
Yao, R., Wang, L., Huang, X., Niu, Y., Chen, Y., Niu, Z., 2018a. The influence of different data and method on estimating the surface urban heat island intensity. Ecol. Indicat. 89, 45–55.
Yao, R., Wang, L., Huang, X., Chen, J., Li, J., Niu, Z., 2018b. Less sensitive of urban surface to climate variability than rural in Northern China. Sci. Total Environ. 628–629, 650–660.
Zhang, X., Friedl, M.A., Schaaf, C.B., Strahler, A.H., Schneider, A., 2004. The footprint of urban climates on vegetation phenology. Geophys. Res. Lett 31 n/a-n/a.
Zhou, J., Chen, Y., Wang, J., Zhan, W., 2011. Maximum nighttime urban heat island (UHI) intensity simulation by integrating remotely sensed data and meteorological observations. IEEE J-STARS 4 (1), 138–146.
Zhou, B., Rybski, D., Kropp, J.P., 2013. On the statistics of urban heat island intensity. Geophys. Res. Lett. 40, 5486–5491.
Zhou, D., Zhang, L., Hao, L., Sun, G., Liu, Y., Zhu, C., 2016a. Spatiotemporal trends of urban heat island effect along the urban development intensity gradient in China. Sci. Total Environ. 544, 617–626.
Zhou, D., Zhang, L., Li, D., Huang, D., Zhu, C., 2016b. Climate–vegetation control on the diurnal and seasonal variations of surface urban heat islands in China. Environ. Res. Lett. 11, 074009.
Zhou, D., Zhao, S., Liu, S., Zhang, L., Zhu, C., 2014. Surface urban heat island in China's 32 major cities: spatial patterns and drivers. Remote Sens. Environ. 152, 51–61.
Zhou, D., Zhao, S., Zhang, L., Liu, S., 2016c. Remotely sensed assessment of urbanization effects on vegetation phenology in China's 32 major cities. Remote Sens. Environ. 176, 272–281.
Zhou, D., Zhao, S., Zhang, L., Sun, G., Liu, Y., 2015. The footprint of urban heat island effect in China. Sci. Rep. 5, 11160.